

Flame retardancy and thermal degradation mechanism of epoxy resin composites based on a DOPO substituted organophosphorus oligomer

Xin Wang^{a,b}, Yuan Hu^{a,c,*}, Lei Song^a, Weiyi Xing^a, Hongdian Lu^a, Pin Lv^d, Ganxin Jie^d

^a State Key Lab of Fire Science, University of Science and Technology of China, Hefei, Anhui 230026, PR China

^b Department of Polymer Science and Engineering, University of Science and Technology of China, Hefei, Anhui 230026, PR China

^c Suzhou Key Laboratory of Urban Public Safety, Suzhou Institute for Advanced Study, University of Science and Technology of China, Suzhou, Jiangsu 215123, PR China

^d State Key Laboratory of Environmental Adaptability for Industrial Products, China National Electric Apparatus Research Institute, Guangzhou 510300, PR China

ARTICLE INFO

Article history:

Received 19 January 2010

Received in revised form

13 March 2010

Accepted 27 March 2010

Available online 6 April 2010

Keywords:

Epoxy resin

Thermal degradation mechanism

Flame retardancy

ABSTRACT

A series of flame-retardant epoxy resins (EP) with different content of poly(DOPO substituted dihydroxyl phenyl pentaerythritol diphosphonate) (PFR) were prepared. The PFR was synthesized via the polycondensation between 10-(2,5-dihydroxyl phenyl)-9,10-dihydro-9-oxa-10-phosphaphenanthrene-10-oxide (DOPO-BQ) and pentaerythritol diphosphonate dichloride (SPDPC). The structure of PFR was confirmed by Fourier transform infrared spectroscopy (FTIR) and ¹H nuclear magnetic resonance (¹H NMR). The flame retardancy and the thermal stability of the EP/PFR hybrids were investigated by limiting oxygen index (LOI) test and thermogravimetric analysis (TGA) in air. The results showed that the incorporation of PFR into EP can improve the thermal stability dramatically. The mechanical results demonstrated that PFR enhanced failure strain slightly accompanied by a decrease in tensile strength. The thermal oxidative degradation mechanisms of the EP/PFR hybrids were investigated by real time Fourier transform infrared spectra (RTFTIR) and direct pyrolysis/mass (DP-MS) analysis. X-ray photoelectron spectroscopy (XPS) was used to explore chemical components of the residual char of EP and EP/PFR hybrid. DP-MS analysis showed that the degradation process of EP/PFR hybrid was divided into two characteristic temperature regions, attributed to the decomposition of phosphate and aromatic structure.

Crown Copyright © 2010 Published by Elsevier Ltd. All rights reserved.

1. Introduction

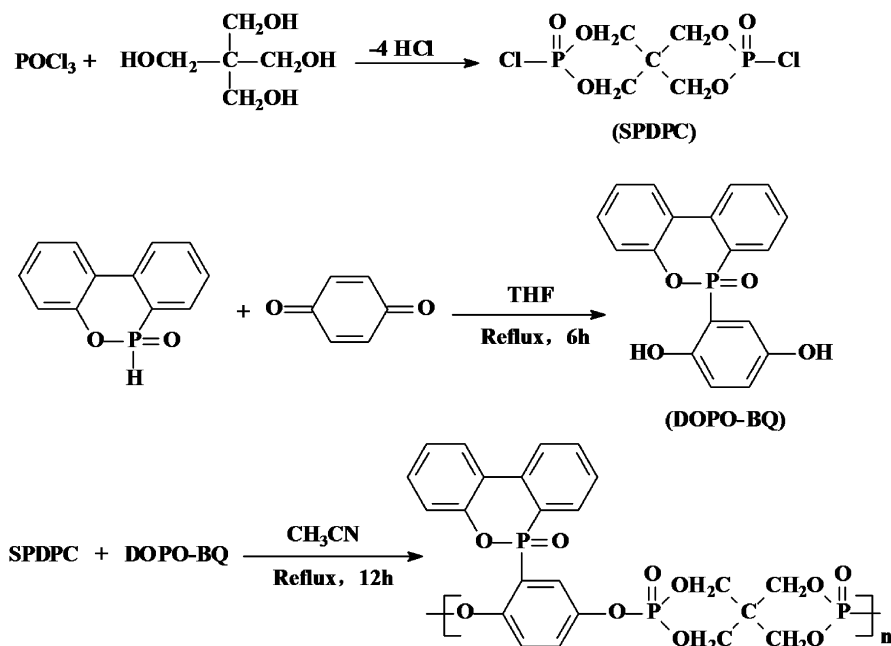
Epoxy resin (EP) is a very important thermosetting material owing to its excellent mechanical and chemical properties. It is used as a high performance material in many fields, such as adhesive, coating, laminating capsulation, electronic/electrical insulation, and composite applications [1–5]. These fields require a remarkable flame-retardant grade, but the flammability is a major drawback of epoxy resin and limits its applications, thus, the flame retardance of EP is an urgent problem and has attracted much attention [6]. Many methods have been developed to improve the flame retardancy of EP. Traditionally, halogenated compounds are widely used as co-monomers or additive with epoxy resins to obtain fire-retardant materials. However, flame-retardant epoxy resins containing bromine or chlorine can produce poisonous and corrosive smoke and may give super-toxic halogenated dibenzodioxins and dibenzofurans [7]. Consequently, to protect the

environment and human health, researchers are focused on exploiting environmental friendly halogen-free fire retardant for epoxy resins. It is reported that epoxy resins can be modified with boron [8], phosphorus [9–13], silicone [14–16], layer double hydroxide [17], melamine [18] and montmorillonite [19], etc. to enhance their flame retardancy. Among them, epoxy resin modified by phosphorus-containing compounds is considered as a promising method due to its high flame-retardant efficiency.

In recent years, 9,10-dihydro-9-oxa-10-phosphaphenanthrene-10-oxide (DOPO) and its derivatives, as a novel kind of phosphorus-containing flame retardants, have received considerable attention due to their high reactivity. The technical literature extensively reports the modification by DOPO as amine curing agents [20], anhydride curing agents [21] and reactive co-monomers [22,23]. Nevertheless, flame retardants modified by DOPO reported above are almost small molecular compounds. The small molecular phosphorus-containing flame retardants display many drawbacks such as leaching and poor compatibility with polymer matrix. The polymeric flame retardant possessed higher phosphorus content and richer aryl group structures than small molecular phosphorus-containing flame retardant reported above and would overcome some shortcomings of low molecular phosphorus-containing flame

* Corresponding author. State Key Lab of Fire Science, University of Science and Technology of China, Hefei, Anhui 230026, PR China. Tel.: +86 551 3601664.

E-mail address: yuanhu@ustc.edu.cn (Y. Hu).



Scheme 1. Synthesis route of SPDPC, DOPO-BQ and PFR.

retardants. The polymeric flame retardant modified by DOPO are seldom reported up to now.

In this paper we presented a thermal and flame-retardant analysis of the epoxy resins blended with different PFR concentrations. The synthesis, characterization, thermal stability and flame-retardant properties of the EP/PFR hybrids were investigated and dynamic FTIR and DP-MS were used to analyze thermal oxidative degradation mechanism of EP/PFR hybrids.

2. Experimental

2.1. Materials

9,10-Dihydro-9-oxa-10-phosphaphenanthrene-10-oxide (DOPO) was supplied by Shandong Mingshan Fine Chemical Industry Co. Ltd (Shandong, China). Epoxy resin (DGEBA, commercial name: E-44) and polyamide (651) were supplied by Hefei Jiangfeng Chemical Industry Co. Ltd (Anhui, China). DOPO, DGEBA and polyamide (651) were all industrial grade. Phosphorus oxychloride was reagent grade and provided by Shanghai HuaYi Group HuaYuan Chemical Industry Co. Ltd (Shanghai, China). Pentaerythritol, p-benzoquinone, tetrahydrofuran (THF), acetonitrile, trichloromethane and diethyl ether were all reagent grade and purchased from Sinopharm Chemical Reagent Co. Ltd (Shanghai, China). THF and acetonitrile were distilled at reduced pressure before use.

Table 1
The composition and LOI values of EP/PFR hybrids with different PFR contents.

Sample	Epoxy resin content (g)	Polyamide 651 content (g)	PFR content (g)	PFR amount (wt%)	LOI (%)
EP	50.0	25.0	0	0	20.5
EP1	50.0	25.0	1.92	2.5	25.0
EP2	50.0	25.0	3.95	5.0	27.6
EP3	50.0	25.0	8.33	10.0	30.2

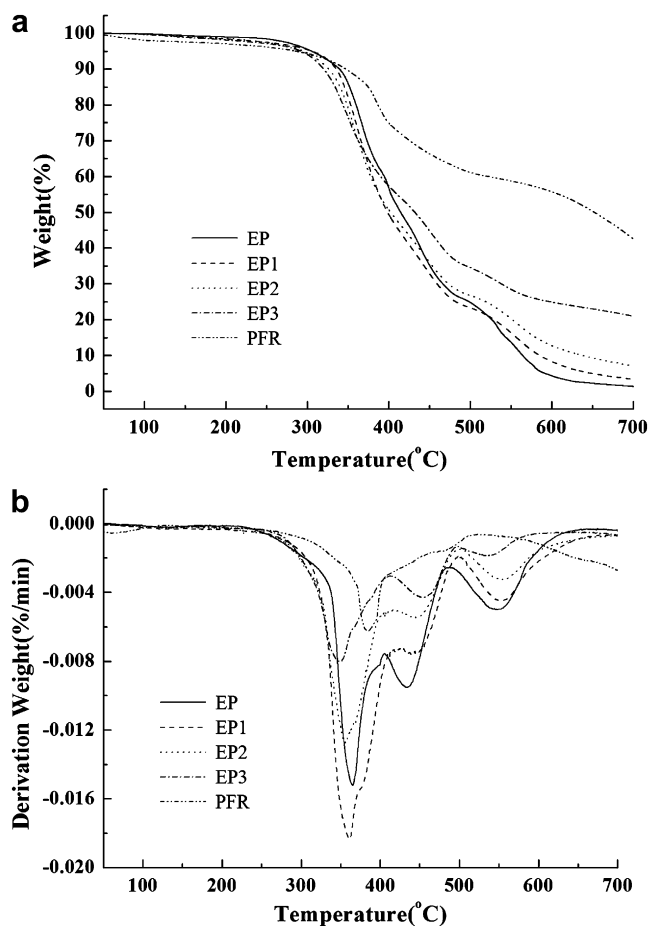


Fig. 1. (a) TG and (b) DTG curves of EP, EP1, EP2, and EP3 in air atmosphere.

Table 2

TG data of PFR, EP and EP/PFR hybrids in air.

Samples	$T_{-5\%}$ (°C)	$T_{-50\%}$ (°C)	T_{\max} (°C)	Char residue (%) at 700 °C
PFR	286	652	384	42.6
EP	305	414	365, 435, 548	1.9
EP1	303	398	360, 442, 556	3.6
EP2	299	402	356, 445, 556	7.3
EP3	291	432	348, 457, 539	20.8

2.2. Synthesis of 10-(2,5-dihydroxyl phenyl)-9,10-dihydro-9-oxa-10-phosphaphenanthrene-10-oxide (DOPO-BQ)

64.8 g of DOPO and 32.4 g of *p*-benzoquinone were dissolved in dried 200 ml THF and then introduced into a three-neck and round-bottom 500 ml glass flask equipped with a nitrogen inlet, a reflux condenser, and a mechanical stirrer. The mixture was stirred and heated slowly to 60 °C for about 1 h under a nitrogen gas atmosphere until DOPO was dissolved completely in THF. The reaction mixture was heated to 72 °C, and then allowed to stir for 6 h under a nitrogen gas atmosphere. After cooling to room temperature, the precipitate was filtered and washed with THF. The white powder was collected by filtration, and dried under reduced pressure. An instrumental analysis of DOPO-BQ was carried out by Fourier transform infrared (FTIR) spectroscopy and ^1H nuclear magnetic resonance (^1H NMR). FTIR (KBr, cm^{-1}): 3418 (Ph-OH), 1596 (P-Ph), 1150 (P=O), 929 (P-O-Ph); ^1H NMR (400 MHz, DMSO- d_6 , ppm): 9.39 (s, 1H, Ph-OH); 9.09 (s, 1H, Ph-OH); 8.25–8.13 (m, 2H, Ph-H); 7.68 (t, 1H, Ph-H); 7.59–7.34 (m, 3H, Ph-H); 7.30–7.17 (m, 2H, Ph-H); 7.12 (dd, 1H, Ph-H); 6.83 (dd, 1H, Ph-H); 6.62–6.53 (m, 1H, Ph-H); 4.29–4.22 (dd, 8H, -OCH₂-).

2.3. Synthesis of pentaerythritol diphosphonate dichloride (SPDPC)

A 500 ml three-neck and round-bottom glass flask equipped with a temperature controller, magnetic stirrer and a reflux condenser was charged with 306 g of phosphorus oxychloride and 49.5 g of pentaerythritol. The temperature of the reaction mixture was raised to 75 °C and maintained for 6 h under a nitrogen gas atmosphere. Afterwards, the reaction mixture was heated slowly to 105 °C and maintained for 12 h. After cooling to room temperature, the precipitate was filtered and washed with trichloromethane and diethyl ether. The white powder was collected by filtration, and dried under reduced pressure. FTIR (KBr, cm^{-1}): 1303 (P=O), 1028 (P-O-C), 583, 541 (P-Cl); ^1H NMR (400 MHz, DMSO- d_6 , ppm): 4.29–4.22 (dd, 8H, -OCH₂-).

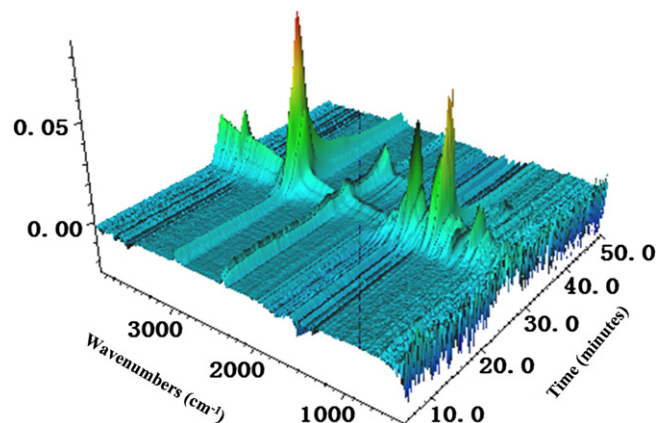
2.4. Synthesis of poly(DOPO substituted dihydroxyl phenyl pentaerythritol diphosphonate) (PFR)

In a 500 ml three-neck and round-bottom glass flask equipped with a temperature controller, magnetic stirrer and a reflux condenser, 29.7 g of SPDPC, 32.4 g of DOPO-BQ and 150 ml acetonitrile were mixed at 70 °C for 1 h. Thereafter, the mixture was

Table 3

Mechanical properties of unmodified and PFR-modified epoxy resins.

Samples	PFR amount (wt%)	Tensile strength (MPa)	Failure strain (%)
EP	0	19.301	0.8
EP1	2.5	19.748	1.6
EP2	5.0	18.423	1.6
EP3	10.0	16.443	1.6

**Fig. 2.** 3D TG-FTIR spectrum of gas phase in the thermal degradation of EP.

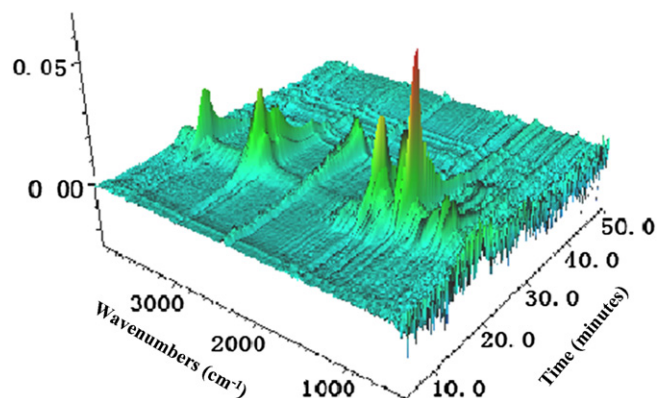
gradually heated and refluxed until no HCl gas was emitted. The solvent was removed by rotary evaporator under reduced pressure. The raw product obtained was washed by acetonitrile three times. The product was then dried in vacuo at 60 °C overnight. FTIR (KBr cm^{-1}): 1596 (P-Ph), 1303, 1150 (P=O), 1028 (P-O-C), 929 (P-O-Ph); ^1H NMR (400 MHz, DMSO- d_6 , ppm): 8.25–8.13 (m, 2H, Ph-H); 7.68 (t, 1H, Ph-H); 7.59–7.34 (m, 3H, Ph-H); 7.30–7.17 (m, 2H, Ph-H); 7.12 (dd, 1H, Ph-H); 6.83 (dd, 1H, Ph-H); 6.62–6.53 (m, 1H, Ph-H), 4.29–4.22 (dd, 8H, -OCH₂-). The synthetic route of above three steps is shown in Scheme 1.

2.5. Preparation of EP/PFR hybrids

Epoxy resin and PFR with the content of 2.5 wt% as total weight were added into a 250 ml three-necked flask equipped with a magnetic stirrer, a thermometer and a reflux condenser. The temperature of the mixture was maintained at 120 °C until PFR was dissolved in epoxy resin completely. The curing agent polyamide (651) was mixed into the EP/PFR with the content of 50 wt% as epoxy resin subsequently. The reaction mixtures were cured in a mould at 60 °C for 1 h. After curing, samples were cooled to room temperature. The composition of EP/PFR hybrids was listed in Table 1. Other samples were synthesized in the same procedures.

2.6. Characterization

All ^1H NMR spectra were performed at on a Bruker AV400 NMR spectrometer (400 MHz) operating in the Fourier transform mode

**Fig. 3.** 3D TG-FTIR spectrum of gas phase in the thermal degradation of EP3.

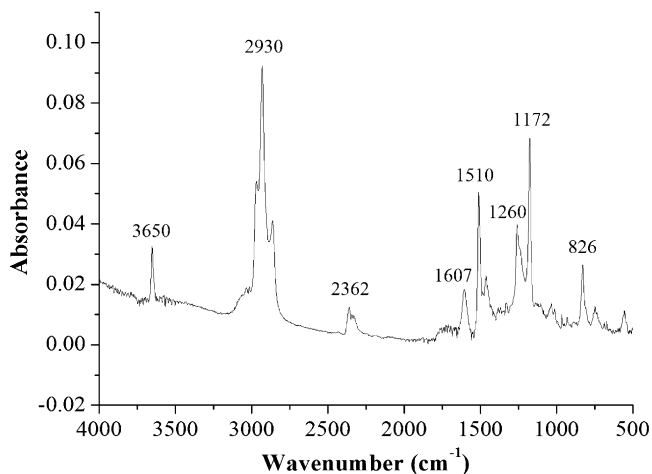


Fig. 4. FTIR spectrum of pyrolysis products for EP at the maximum decomposition rate (27.6 min).

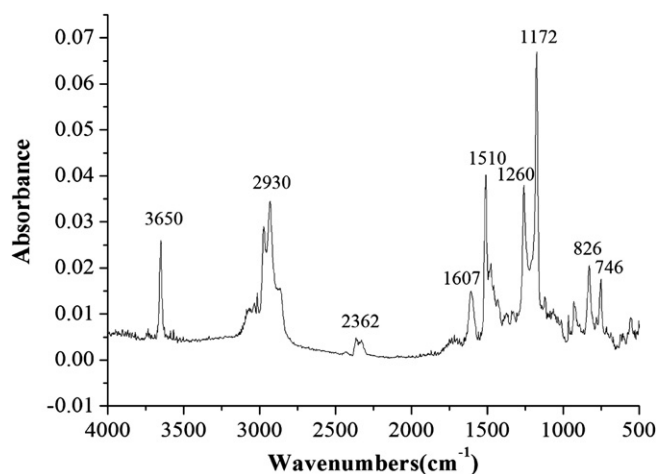


Fig. 5. FTIR spectrum of pyrolysis products for EP3 at the maximum decomposition rate (19.5 min).

using DMSO- d_6 as solvent. The thermogravimetric analysis (TGA) of samples were carried out with Q5000 thermal analyzer (TA Co., USA) from 50 °C to 700 °C at a heating rate of 20 °C/min. The limiting oxygen index (LOI) was measured according to ASTM D2863. The apparatus used was an HC-2 oxygen index meter (Jiangning Analysis Instrument Company, China). The specimens used for the test were of dimensions $100 \times 6.5 \times 3 \text{ mm}^3$. The real time Fourier transform infrared spectra (RTFTIR) were recorded using a Nicolet MAGNA-IR 750 spectrophotometer equipped with a heating device and a temperature controller. Powders of samples were mixed with KBr powders, and the mixture was pressed into a tablet, which was then placed in a ventilated oven. The temperature of the oven was raised at a heating rate of 10 °C/min. The

dynamic FTIR spectra were obtained in situ during the thermo-oxidative degradation processes. Thermogravimetric analysis/infrared spectrometry (TG-IR) of the samples was performed using the TGA Q5000 IR thermogravimetric analyzer that was interfaced to the Nicolet 6700 FTIR spectrophotometer. About 5.0 mg of the sample was put in an alumina crucible and heated from 30 to 600 °C at a heating rate of 20 °C/min (nitrogen atmosphere, flow rate of 45 ml/min). DP-MS analysis was carried out with a Micro-mass GCT-MS spectrometer using the standard direct insertion probe for solid polymer materials, at a heating rate of 10 °C min⁻¹ in the range of 30–600 °C. The mass data were continuously acquired at a scan rate of 0.1 s. Electron impact (EI) was used for the mass spectra with 70 eV and the mass range of 10–1000 m/z . All

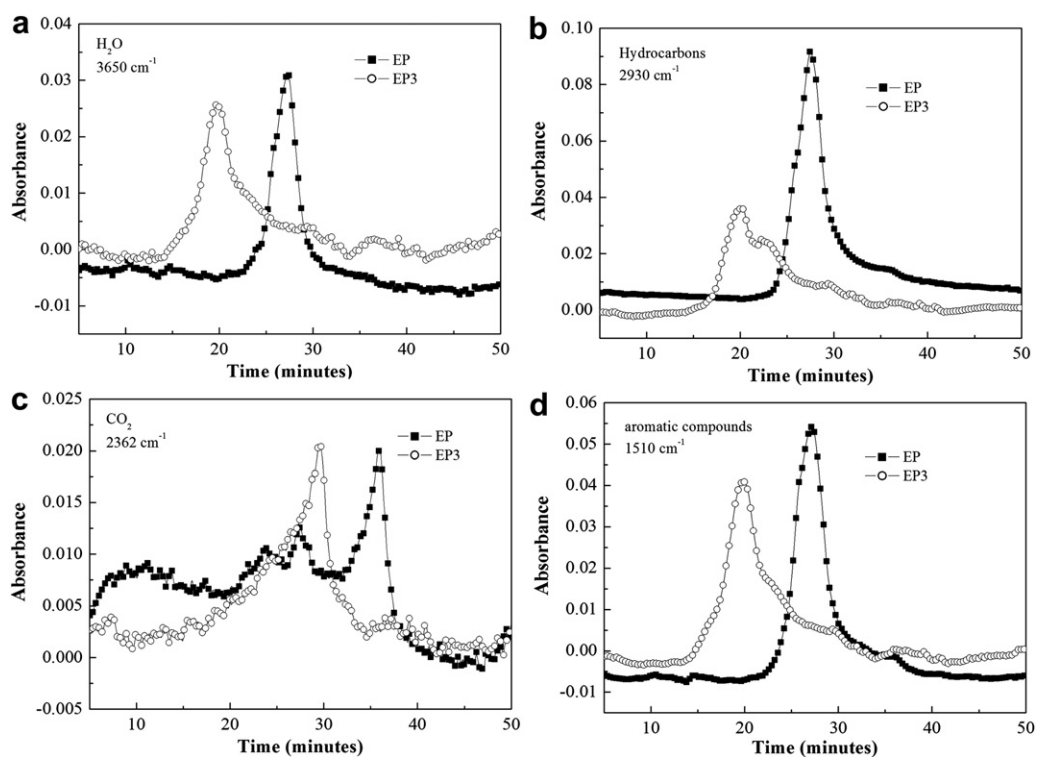


Fig. 6. Absorbance of pyrolysis products for EP and EP3 vs time: (a) H₂O; (b) hydrocarbons; (c) CO₂; and (d) aromatic compounds.

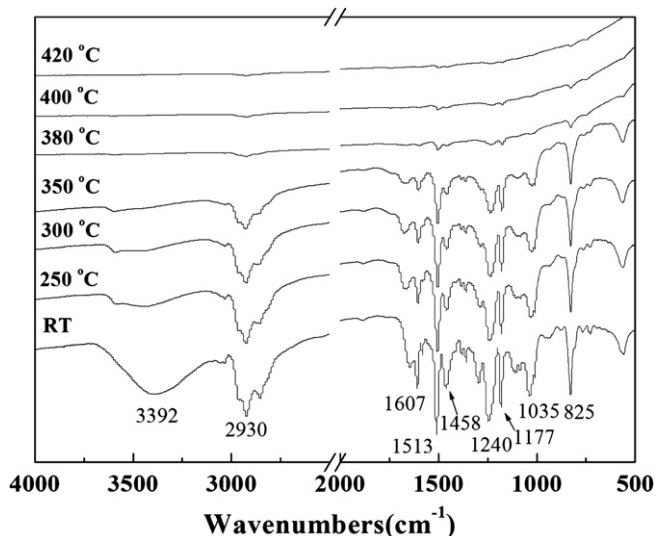


Fig. 7. The dynamic FTIR spectra of EP at different pyrolysis temperatures.

pyrolysis products were identified using the software of the mass spectrometer or by comparison with mass spectra in the literature. X-ray photoelectron spectroscopy (XPS) spectra of the char residue was recorded with a VG Escalab Mark II spectrometer (VG Scientific Ltd, UK), using Al K α excitation radiation ($h\nu = 1253.6$ eV). Mechanical properties of flame-retardant EP were tested with a WSM-20KB universal testing machine (Changchun, China) according to GB/T1040-92.

3. Results and discussion

3.1. Flame-retardant properties and thermal stability of EP and EP/PFR hybrids

The LOI values of EP and EP/PFR hybrids are given in Table 1. Table 1 presents that a higher LOI value is obtained with the increase in phosphorus content. LOI increases drastically from 20.5 to 30.2 (meets the flame-retardant criterion) when PFR content is increased from 0 to 10 wt %. The results indicate that PFR exhibits good flame-retardant effect to epoxy resin.

The TG and DTG curves of PFR, EP and EP/PFR hybrids in air atmosphere are shown in Fig. 1a and b. The onset degradation temperature (T_d) of samples which is evaluated by the temperature of 5 wt% weight loss ($T_{-5\%}$), the mid-point temperature of the degradation ($T_{-50\%}$), and the solid residue at 700 °C are obtained from the TG curves; the temperature of the maximum weight loss rate (T_{max}) of samples is obtained from the DTG curves. These data are listed in Table 2.

As can be seen from Fig. 1, PFR has one stage of weight loss, and accordingly there is only one differential thermogravimetric (DTG) peak. PFR begins to degrade at 286 °C, and the maximum mass loss rate occurs at about 384 °C. The stable solid residue at 700 °C is about 42.6 wt%. The T_d of PFR is lower than that of pure epoxy resin, which may be attributed to the fact that the O=P–O bond in PFR is less stable than the common C–C bond. Therefore, the T_d of EP/PFR hybrids trends to decrease gradually with the increase of the PFR addition.

As for pure EP, the thermal oxidative degradation process has three stages. The first stage is in the temperature range of 180–410 °C corresponding to a strong DTG peak at 365 °C (T_{max1}) and the weight loss is 47.9%. These indicate that some complex chemical reactions take place at the first stage of thermal oxidative

Table 4
Assignment of FTIR spectra of EP and EP3.

Wavenumber (cm ⁻¹)	Assignment
<i>EP</i>	
3392	O–H stretching vibration of water or phenol
2930	–CH ₃ and –CH ₂ – stretching vibration
1607, 1513, 1458	C–C stretching vibration of aromatic ring
1291	–CH ₂ – bending vibration
1240, 1035	C–H vibration of –C ₆ H ₄ –O–CH ₂ –
1177	C–O stretching vibration
<i>EP/PFR hybrids</i>	
3392	O–H stretching vibration of water or phenol
2930	–CH ₃ and –CH ₂ – stretching vibration
1607, 1513, 1458	C–C stretching vibration of aromatic ring
1291	–CH ₂ – bending vibration or P=O stretching vibration
1240, 1035	C–H vibration of –C ₆ H ₄ –O–CH ₂ –
1177	C–O and/or P–O–Ph stretching vibration
1458	P–Ph stretching vibration

degradation, including the free radical chain scission of the isopropylidene linkage and the branching and crosslinking reactions of molecular chains induced by oxygen, besides the elimination of the hydration water. The second and third stage are in the temperature ranges of 410–490 °C and 490–660 °C corresponding to T_{max2} , T_{max3} of 435 °C, 548 °C, respectively. During the two stages, the macromolecular chains of EP are further oxidized and many small molecular degradation products are released.

Fig. 1a and b also shows TG and DTG curves of the EP1, EP2 and EP3 in air, respectively. The thermal oxidative degradation process of all the hybrid samples has the similar three stages as the pristine EP. It can be seen that PFR has remarkable influence on the thermal degradation of EP. EP/PFR hybrids decompose faster compared with EP at lower temperature. At higher temperature, $T_{50\%}$ of the EP1, EP2 is lower than that of EP, whereas $T_{50\%}$ of the EP3 is higher than that of EP. As the PFR content increases, the residue left at 700 °C increases significantly. Moreover, the char yield at 700 °C for EP3 is 20.8% which is much higher than that of EP. These indicate that the incorporation of PFR can improve the degradation stability of the EP/PFR hybrids at higher temperature and promote the formation of char residue.

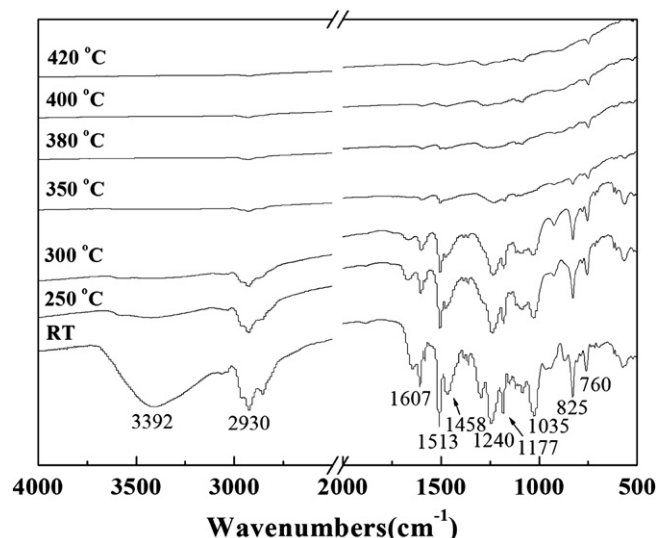


Fig. 8. The dynamic FTIR spectra of EP3 at different pyrolysis temperatures.

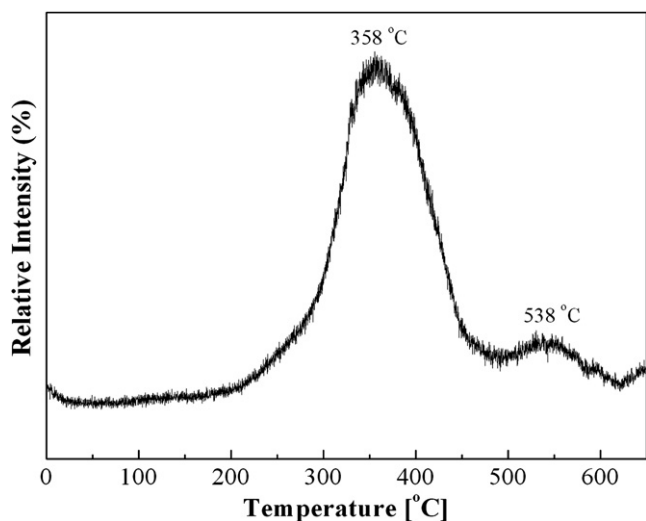


Fig. 9. Total ion current (TIC) curve of the decomposition process of EP3.

3.2. Mechanical properties

The data for the tensile strength, and failure strain of the unmodified and PFR-modified epoxy resins were obtained from the computer controlled universal tensile testing machine. The results for the mechanical properties are summarized in Table 3. It can be seen that the tensile strength strain can be slightly enhanced by the addition of PFR with appropriate contents (2.5 wt%). The incorporation of PFR gives reinforcement impact on the EP firstly. Nevertheless, the tensile strength of EP/PFR hybrids begins to decrease at higher PFR load. As is known, the phosphorus-containing flame retardant at high content usually cause a negative impact on the mechanical properties of the polymer matrix. This phenomenon is also reported by earlier literatures [1,24]. Moreover, the PFR-modified epoxy resins exhibit relatively ductile behaviors compared to the unmodified ones.

3.3. TG-FTIR analysis of EP and EP/PFR hybrids

TG-FTIR was used to analyze the gas products during the thermal degradation. The 3D TG-FTIR spectra of gas phase in the thermal degradation of EP and EP3 are shown in Figs. 2 and 3.

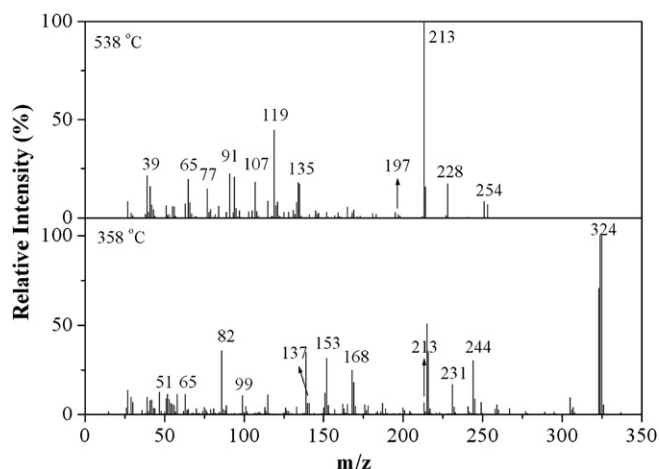


Fig. 10. EI-MS spectra of compounds evolved from EP3 at different temperatures.

In Fig. 2, peaks in the regions of around $3600\text{--}3700\text{ cm}^{-1}$, around $2750\text{--}3150\text{ cm}^{-1}$, around $2250\text{--}2400\text{ cm}^{-1}$, around $1400\text{--}1650\text{ cm}^{-1}$, and around $1100\text{--}1300\text{ cm}^{-1}$ are noted. Some of the gaseous decomposition products of the EP materials were unambiguously identified by characteristic strong FTIR signals, such as methane (3015 cm^{-1}), and water (3650 cm^{-1}) [25]. The main share of the bands of the decomposition products is attributed to the functional groups with characteristic, unambiguous band positions: compounds containing aromatic ring ($1607, 1510\text{ cm}^{-1}$) and phenol (746 cm^{-1}), and methyl-substituted compounds (2930 cm^{-1}) [25–27].

FTIR spectra of pyrolysis products of EP at maximum decomposition rates are shown in Fig. 4. The main products of the thermal decomposition of EP are compounds containing --OH (such as H_2O , phenol; $3500\text{--}3600\text{ cm}^{-1}$), CO_2 (2360 cm^{-1}), aromatic ethers (1260 cm^{-1}), hydrocarbons (C--H stretching at 1172 cm^{-1}), compounds containing aromatic rings ($1607, 1510\text{ cm}^{-1}$), etc [25–27]. It is well-known that depolymerization is the main process associated with the thermal degradation of polymers. In the process of depolymerization, the main decomposition products are CO_2 , phenol, and hydrocarbons, etc.

Fig. 3 shows the 3D TG-FTIR spectrum of gas phase in the thermal degradation of EP3. As shown in Fig. 5, the evolved gas analysis for EP3 at maximum decomposition rates exhibited characteristic bands of H_2O and/or phenol (3650 cm^{-1}), CO_2 (2362 cm^{-1}), hydrocarbons (--CH_3 and $\text{--CH}_2\text{--}$ groups: $2950\text{--}2850$ and $1100\text{--}1300\text{ cm}^{-1}$) and compounds containing aromatic rings ($1607, 1510\text{ cm}^{-1}$) [25–27] which is similar to that of EP. In fact, the new absorption band at 924 cm^{-1} appears which is due to the structures containing --P--O--Ph . Moreover, it is probably that other new absorption bands, such as 1260 cm^{-1} (P=O), 1118 cm^{-1} (--P--O--P--O), almost coincides with the characteristic peaks of the EP matrix. It can be concluded that the polyphosphate structures are formed by decomposition of PFR. These polyphosphate structures can react with other pyrolysis products (such as phenol or bisphenol) to form the P--O--Ph bond.

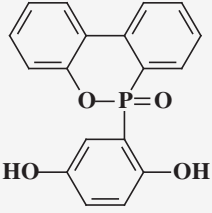
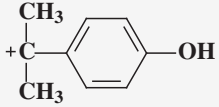
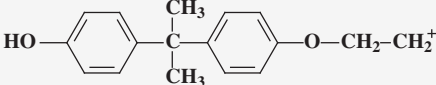

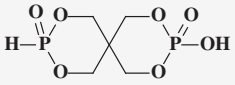
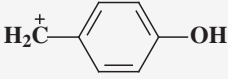
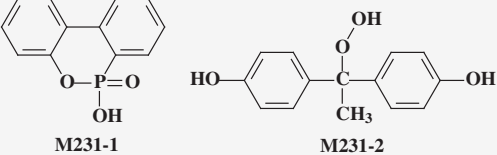
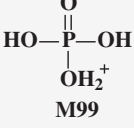
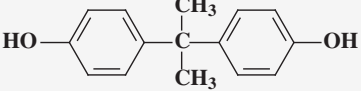
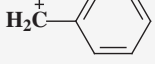
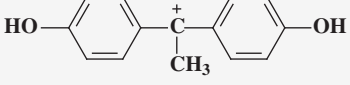
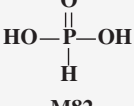
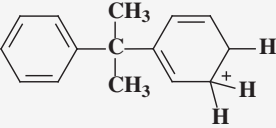
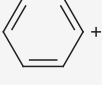
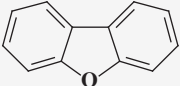

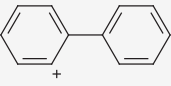
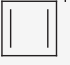
The absorbance of pyrolysis products for EP and EP3 vs time is revealed in Fig. 6. It can be seen that the pyrolysis products for EP3 begin to release at about 15 min, whereas those for EP begins to release at about 23 min. It can be interpreted that PFR can catalyze the thermal decomposition of EP. However, the absorbance intensity of pyrolysis products for EP3 is lower than that for EP, especially hydrocarbons. Consequently, the addition of PFR can reduce the release of combustible gas and the weight loss. The results of the pyrolysis products release correspond well to thermal analysis and are explained by the proposed decomposition models discussed below.

3.4. Thermal degradation of EP and EP/PFR hybrids

Dynamic FTIR was employed to evaluate the solid pyrolysis products of EP and EP3. The FTIR spectra of EP at different degradation temperatures are shown in Fig. 7. The assignment of dynamic FTIR spectra of EP and EP3 is presented in Table 4. It can be seen that peaks at $3392, 2930, 1607, 1513, 1458, 1240, 1177$ and 1035 cm^{-1} are the characteristic absorptions of EP. The band at 3392 cm^{-1} nearly disappears at the temperature of $250\text{ }^\circ\text{C}$, and this can be explained by the release of water. The relative intensities of other characteristic peaks do not change below $350\text{ }^\circ\text{C}$. While the temperature rises up to $380\text{ }^\circ\text{C}$, it's found that the absorption peaks at $2930, 1607, 1458, 1240$ and 1035 cm^{-1} disappear, indicating that the main decomposition happens at this stage. This is consistent with the TGA results.


The FTIR spectra of the EP3 at different degradation temperatures are shown in Fig. 8. The FTIR spectrum of EP3 shows very

Table 5
Structural assignments in the DP-MS of EP3.

<i>m/z</i>	Structure	<i>m/z</i>	Structure
324	 M324	135	 M135
254	 M254	119	 M119-1 M119-2
244	 M244	107	 M107
231	 M231-1 M231-2	99	 M99
228	 M228	91	 M91
213	 M213	82	 M82
197	 M197	77	 M77
168	 M168	65	 M65
153	 M153	51	 M51

(continued on next page)

Table 5 (continued)

m/z	Structure	m/z	Structure
137	$\begin{array}{c} \text{CH}_2\text{OH} \\ \\ \text{HOCH}_2-\text{C}-\text{CH}_2\text{OH}_2^+ \\ \\ \text{CH}_2\text{OH} \\ \text{M137} \end{array}$	39	 M39

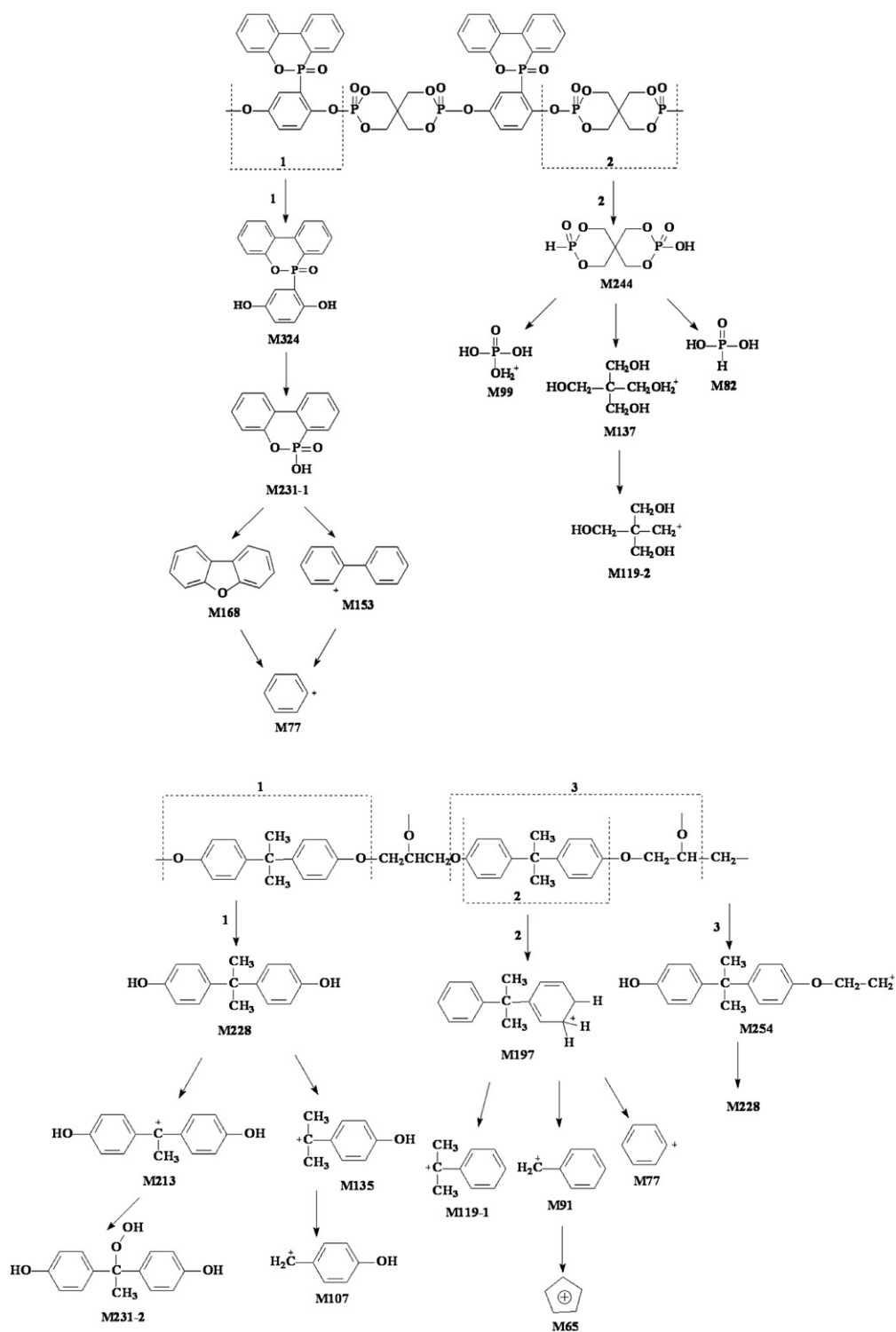


Fig. 11. Oversimplified mass fragmentations of EP3.

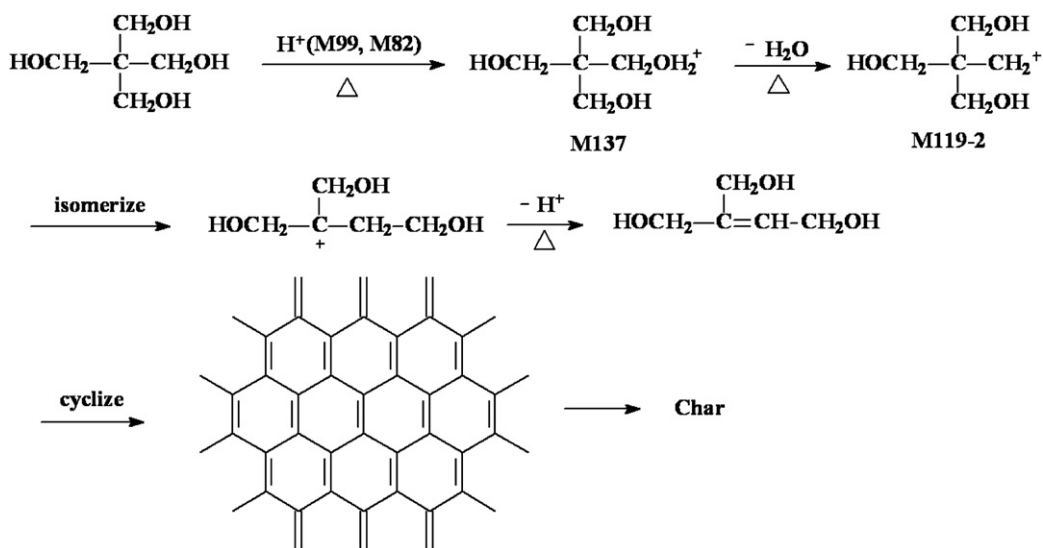


Fig. 12. Schematic outline of the degradation process of EP/PFR hybrids.

similar features to that of EP. In this figure, the characteristic peaks of PFR are not obvious because its characteristic bands probably coincide with the characteristic bands of the EP matrix. It is worth noting that at 350 °C the intensities of most peaks decrease sharply, which means that the presence of PFR catalyzes the thermal degradation of EP and formation of char. The residual char can prevent the materials from further degradation during combustion. This conclusion is also suggested by the TG-FTIR analysis above.

3.5. DP-MS analysis of EP and EP/PFR hybrids

Fig. 9 shows the total ion current (TIC) chromatogram of EP3 by DP-MS. It can be observed that the EP3 has two TIC peaks at 358 and 538 °C. The mass spectra corresponding to the TIC peaks at different temperatures are presented in Fig. 10 and the products identified are listed in Table 5 [28].

The first peak at around 358 °C in the mass spectrum is mainly attributed to the decomposition products of PFR, such as 324m/z for

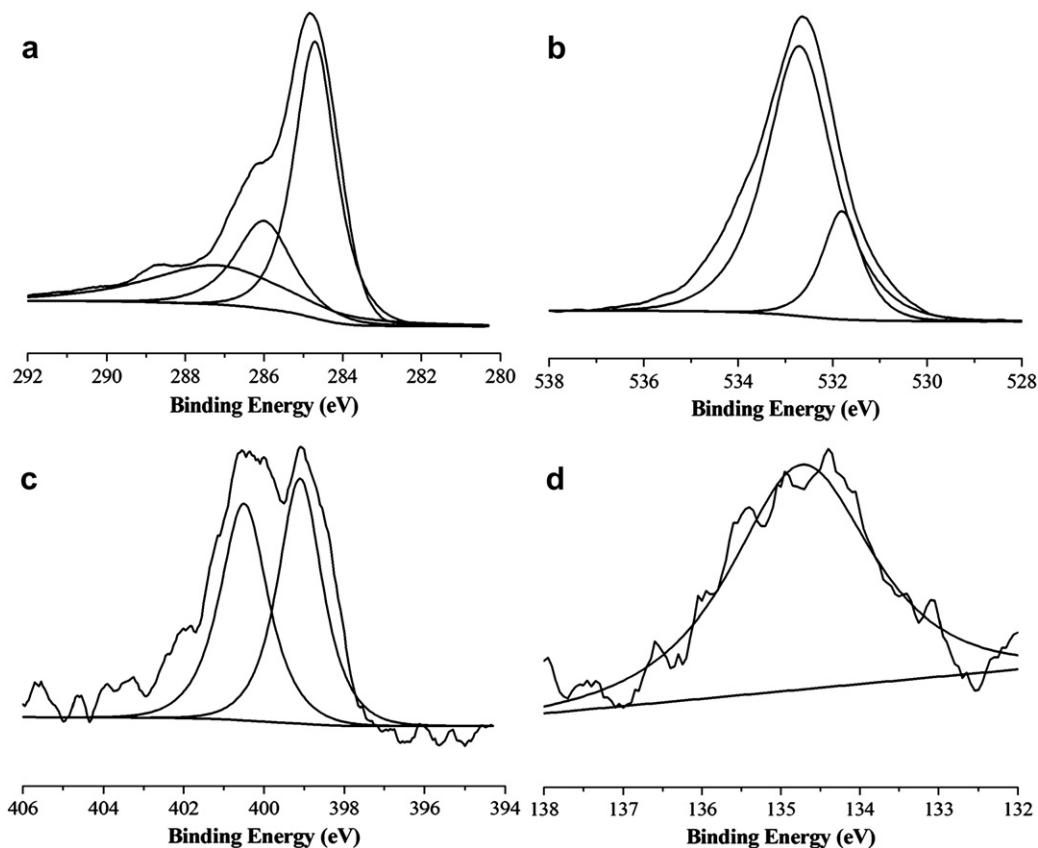


Fig. 13. (a) C_{1s}, (b) O_{1s}, (c) N_{1s} and (d) P_{2p} XPS spectra of the char residue of EP.

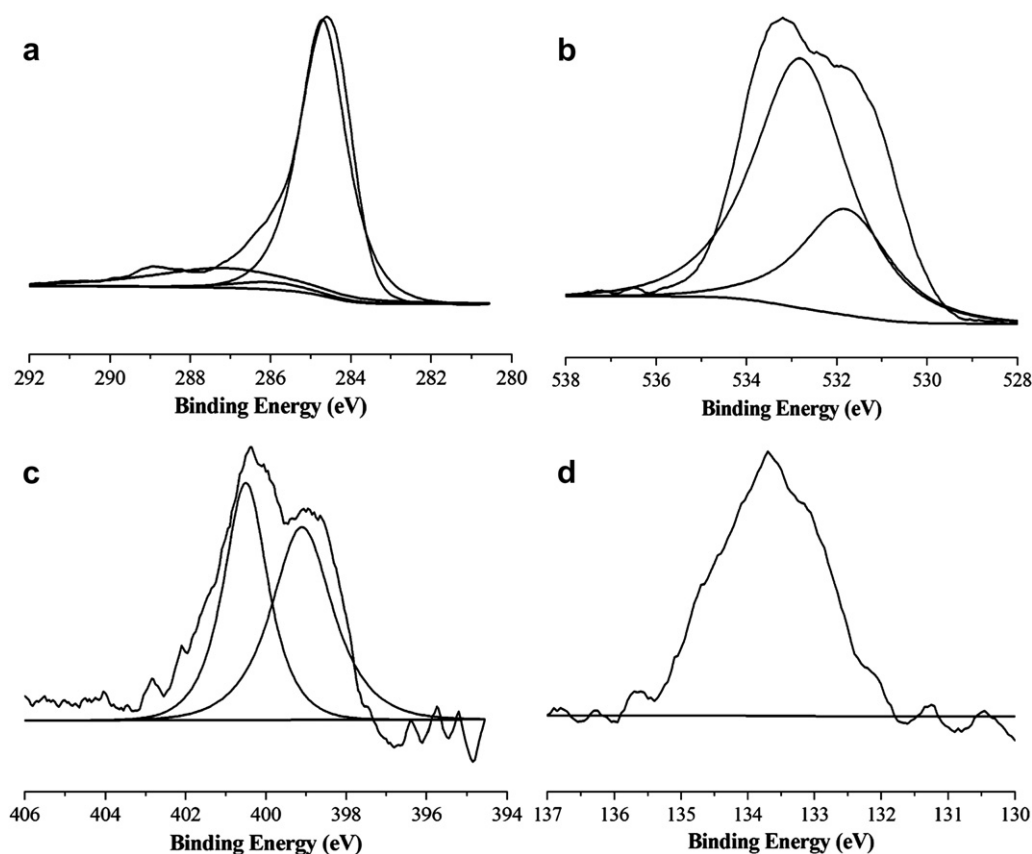


Fig. 14. (a) C_{1s} , (b) O_{1s} , (c) N_{1s} and (d) P_{2p} XPS spectra of the char residue of EP3.

$C_{18}H_{13}O_4P$ and $224m/z$ for $C_5H_{10}O_7P_2$. And the peaks at $99m/z$ and $82m/z$ are due to the degradation of phosphate. In the mass spectrum at $538^\circ C$, two new strong peaks at $119m/z$ corresponding to the mixture ions of M119-1 and M119-2, and $213m/z$ corresponding to M213 appear. And the peaks at $254m/z$ for M254, $228m/z$ for M228, and $135m/z$ for M135 can be assigned to the fragment ions that mainly resulted from the degradation of epoxy resin matrix.

The oversimplified fragment of EP3 is shown in Fig. 11 with the data from the mass fragmentations of the key TIC ions shown collectively in Fig. 10. Associating with the former paragraph as has been discussed, it can be found that the degradation of EP3 can be divided into two steps. From 300 to $400^\circ C$, the degradation is mainly attributed to phosphate groups and mostly carbonyl group in the PFR. When raising temperature over $450^\circ C$, alkyl chain and some aromatic molecules of epoxy resin matrix are decomposed.

Therefore, on the basis of the results for volatile pyrolysis products and residue pyrolysis products, a possible route of the degradation process of EP/PFR hybrids, as shown in Fig. 12 [29], has been postulated and summarized for the main decomposition pathway for EP3.

3.6. Chemical components of the residual char of EP and EP/PFR hybrids

The chemical components of the residual char for EP and EP3 (heated in muffle furnace for 10 min at $600^\circ C$) were investigated by XPS. As shown in Figs. 13 and 14, three bands are observed from C_{1s} spectra: the peak at around 284.7 eV is attributed to C–H and C–C in aliphatic and aromatic species, the peak at around 286.0 eV is assigned to C–O (ether and/or hydroxyl group), and another peak at around 287.2 eV corresponded to carbonyl groups [30]. O_{1s}

spectrum has two peaks at around 531.8 and 532.7 eV. It is reported that the peak at 531.8 eV can be attributed to the =O in phosphate or carbonyl groups and the peak centered at 532.7 eV is assigned to –O– in C–O–C, C–O–P, and/or C–OH groups [26]. For the N_{1s} spectra, the peak at 399.1 eV can be assigned the nitrogen in imide groups formed by the condensation of low molecular polyamide curing agent at higher temperature. The peak at 400.5 eV corresponds to formation of some oxidized nitrogen compounds. The single peak between 134 and 135 eV in P_{2p} spectrum can be assigned to the pyrophosphate and/or polyphosphate [26,31].

From Table 6, it can be found that the addition of PFR influences the flame retardancy and thermal degradation of the composites greatly. The atom percent of carbon in the char residues of EP and EP3 is 50.91% and 76.94% , respectively. And the atom percent of oxygen in the char residues of EP3 is lower than that in the char residue of EP. These mean that the incorporation of PFR into EP can

Table 6
XPS results of the residual char of EP and EP3.

System	Binding energy (eV)	Atom (%)
EP		
C_{1s}	284.7, 286.0, 287.2	50.91
O_{1s}	531.8, 532.7	38.79
N_{1s}	399.1, 400.5	2.81
P_{2p}	134.7	0.05
EP3		
C_{1s}	284.7, 286.0, 287.2	76.94
O_{1s}	531.8, 532.8	19.23
N_{1s}	399.1, 400.5	2.76
P_{2p}	133.8	1.07

promote the formation of char residues and enhance the thermal oxidative resistance of the EP matrix. The effect of PFR on combustion behaviors could be summarized as follows: under the high temperature, PFR can increase the char yield remarkably and improve the thermal oxidative stability of the char layer. The char layer builds up on the surface of the burning polymer, insulates the heat transformation and the dispersion of oxygen into underlying polymeric substrate, and prevents the release of volatile products of underlying polymeric substrate from the matrix. Thus, the combustion is retarded.

4. Conclusions

A series of epoxy resin/PFR hybrids containing 0 wt%, 2.5 wt%, 7.5 wt% and 10 wt% content of PFR were prepared. The high phosphorus content and rich aryl group structures of PFR contribute an excellent flame retardancy to epoxy resins without a considerable decrease of the mechanical properties. EP/PFR hybrids possess lower initial decomposition temperatures and higher char residues than pure EP. The degradation of EP/PFR hybrids can be divided into two main steps. The first stage can be assigned to the decomposition of phosphate and carbonyl group in the PFR, whereas the second is due to the thermal pyrolysis of alkyl chains and some aromatic structures. The degradation products of PFR, including pentaerythritol (carbon agent), phosphorus acid and phosphoric acid or poly(phosphoric acid) (acid source), associate with amine curing agent (blowing agent) to constitute a intumescent flame-retardant system. Thus, the intumescent char layer is formed to protect the inner polymer matrix.

Acknowledgements

The work was financially supported by the Program for Specialized Research Fund for the Doctoral Program of Higher Education (200803580008), the National Natural Science Foundation of China (no. 50903080) and the Program for Science and Technology of SuZhou (SG-0841), the Opening Project of State Key

Laboratory of Environmental Adaptability for Industrial Product, and the Program for the graduate innovation fund in University of Science and Technology of China.

References

- [1] Chen ZK, Yang G, Yang JP, Fu SY, Ye L, Huang YG. *Polymer* 2009;50(5):1316–23.
- [2] Wu CS, Liu YL, Chiu YC, Chiu YS. *Polym Degrad Stab* 2002;78(1):41–8.
- [3] Baller J, Becker N, Ziehmer M, Thomassey M, et al. *Polymer* 2009;50(14):3211–9.
- [4] Morell M, Ramis X, Ferrando F, Yu YF, Serra A. *Polymer* 2009;50(23):5374–83.
- [5] Chen ZK, Yang JP, Ni QQ, Fu SY, Huang YG. *Polymer* 2009;50(19):4753–9.
- [6] Lin CH, Lin HT, Chang SL, Hwang HJ, Hu YM, Taso YR, et al. *Polymer* 2009;50(10):2264–72.
- [7] Liu R, Wang XD. *Polym Degrad Stab* 2009;94(4):617–24.
- [8] Martin C, Lligadas G, Ronda JC, Galia M, Cadiz V. *J Polym Sci: Polym Chem* 2006;44(21):6332–44.
- [9] Lin CH, Hwang TY, Taso YR, Lin TL. *Macromol Chem Phys* 2007;208(24):2628–41.
- [10] Wu CS, Liu YL, Chiu YS. *Polymer* 2002;43(15):4277–84.
- [11] Li X, Ou YX, Shi YS. *Polym Degrad Stab* 2002;77(3):383–90.
- [12] Hergenrother PM, Thompson CM, Smith JG, Connell JW, Hinkley JA, Lyon RE, et al. *Polymer* 2005;46(14):5012–24.
- [13] Shieh JY, Wang CS. *Polymer* 2001;42(18):7617–25.
- [14] Zheng Y, Chonung K, Jin XL, Wei P, Jiang PK. *J Appl Polym Sci* 2008;107(5):3127–36.
- [15] Mercado LA, Galia M, Reina JA. *Polym Degrad Stab* 2006;91(11):2588–94.
- [16] Liu YL, Chang GP, Wu CS. *J Appl Polym Sci* 2006;102(2):1071–7.
- [17] Tseng CH, Hsueh HB, Chen CY. *Compos Sci Technol* 2007;67(11):2350–62.
- [18] Toldy A, Toth N, Anna P, Marosi G. *Polym Degrad Stab* 2006;91(3):585–92.
- [19] Guo BC, Jia DM, Cai CG. *Eur Polym J* 2004;40(8):1743–8.
- [20] Artner J, Ciesielski M, Walter O, Doring M, Perez RM, Sandler JKW, et al. *Macromol Mater Eng* 2008;293(6):503–14.
- [21] Lin CH, Wu CY, Wang CS. *J Appl Polym Sci* 2000;78(1):228–35.
- [22] Liu YL. *J Polym Sci: Polym Chem* 2002;40(3):359–68.
- [23] Wang CS, Shieh JY. *J Appl Polym Sci* 1999;73(3):353–61.
- [24] Li B, He JM. *Polym Degrad Stab* 2004;83(2):241–6.
- [25] Braun U, Balabanovich AI, Schartel B. *Polymer* 2006;47(26):8495–508.
- [26] Wu K, Hu Y, Song L, Lu HD, Wang ZZ. *Ind Eng Chem Res* 2009;48(6):3150–7.
- [27] Wu K, Song L, Hu Y, Lu HD, Kandola BK, Kandare E. *Prog Org Coat* 2009;65(4):490–7.
- [28] Huang ZG, Shi WF. *Polym Degrad Stab* 2006;91(8):1674–84.
- [29] Wang ZY, Han EH, Ke W. *Prog Org Coat* 2005;53(1):29–37.
- [30] Song L, He QL, Hu Y, Chen H, Liu L. *Polym Degrad Stab* 2008;93(3):627–39.
- [31] Wang JS, Wang DY, Liu Y. *J Appl Polym Sci* 2008;108(4):2644–53.